Physiologia Plantarum 133: 92–105. 2008

Inorganic carbon acquisition in potentially toxic and non-toxic diatoms: the effect of pH-induced changes in seawater carbonate chemistry

Scarlett Trimborn[a,*], Nina Lundholm[b], Silke Thoms[a], Klaus-Uwe Richter[a], Bernd Krock[a], Per Juel Hansen[b] and Björn Rost[a]

[a]Alfred Wegener Institute for Polar and Marine Research, Am Handelshafen 12, 27570 Bremerhaven, Germany
[b]Marine Biological Laboratory, University of Copenhagen, Strandpromenaden 5, DK-3000 Helsingør, Denmark

Correspondence
*Corresponding author,
e-mail: scarlett.trimborn@awi.de

Received 12 July 2007; revised 21 November 2007

doi: 10.1111/j.1399-3054.2007.01038.x

The effects of pH-induced changes in seawater carbonate chemistry on inorganic carbon (C_i) acquisition and domoic acid (DA) production were studied in two potentially toxic diatom species, *Pseudo-nitzschia multiseries* and *Nitzschia navis-varingica*, and the non-toxic *Stellarima stellaris*. In vivo activities of carbonic anhydrase (CA), photosynthetic O_2 evolution and CO_2 and HCO_3^- uptake rates were measured by membrane inlet MS in cells acclimated to low (7.9) and high pH (8.4 or 8.9). Species-specific differences in the mode of carbon acquisition were found. While extracellular carbonic anhydrase (eCA) activities increased with pH in *P. multiseries* and *S. stellaris, N. navis-varingica* exhibited low eCA activities independent of pH. Half-saturation concentrations ($K_{1/2}$) for photosynthetic O_2 evolution, which were highest in *S. stellaris* and lowest in *P. multiseries*, generally decreased with increasing pH. In terms of carbon source, all species took up both CO_2 and HCO_3^-. $K_{1/2}$ values for inorganic carbon uptake decreased with increasing pH in two species, while in *N. navis-varingica* apparent affinities did not change. While the contribution of HCO_3^- to net fixation was more than 85% in *S. stellaris*, it was about 55% in *P. multiseries* and only approximately 30% in *N. navis-varingica*. The intracellular content of DA increased in *P. multiseries* and *N. navis-varingica* with increasing pH. Based on our data, we propose a novel role for eCA acting as C_i-recycling mechanism. With regard to pH-dependence of growth, the 'HCO_3^- user' *S. stellaris* was as sensitive as the 'CO_2 user' *N. navis-varingica*. The suggested relationship between DA and carbon acquisition/C_i limitation could not be confirmed.

Introduction

Marine diatoms are key players in the ocean carbon cycle, accounting for at least 40% of the marine primary production (Nelson et al. 1995). Until recently, the effect of inorganic carbon availability on photosynthesis has been largely ignored in marine phytoplankton ecology,

Abbreviations – *a*, fractional contribution of HCO_3^- to total C_i uptake; CA, carbonic anhydrase; CCM, carbon-concentrating mechanism; C_i, inorganic carbon; 'CO_2 user', algae predominantly taking up CO_2; DA, domoic acid; DBS, dextran-bound sulphonamide (inhibitor for eCA); DIC, dissolved inorganic carbon; eCA, extracellular CA; ε_a, fractionation factor between CO_2 and HCO_3^-; ε_b, fractionation factor of HCO_3^- and CO_3^{2-}; ε_f, intrinsic fractionation factor for RubisCO; ε_p, isotope fractionation during POC formation; ε_s, equilibrium discrimination between CO_2 and HCO_3^-; 'HCO_3^- user', algae predominantly taking up HCO_3^-; iCA, intracellular CA; $K_{1/2}$, half-saturation concentration; L, leakage (CO_2 efflux : gross C_i uptake); MIMS, membrane inlet mass spectrometer; POC, particulate organic carbon; PGA, 3-phosphoglyleric acid; RubisCO, ribulose-1,5-bisphosphate carboxylase/oxygenase; V_{max}, maximum rates (substrate saturated).

particularly because dissolved inorganic carbon (DIC) is always in excess relative to other nutrients. In seawater, C_i is mainly found in the form of HCO_3^- (approximately 2 mmol l^{-1}) but also comprises low and variable concentrations of dissolved CO_2 (approximately 5–25 μmol l^{-1}). The pH, which reflects the partitioning of the carbon species, is usually about 8.2 in air-equilibrated surface waters. Elevated pH in ocean surface waters is mainly caused by intense primary production during periods with high concentrations of phytoplankton cells, e.g. towards the end of bloom periods (Hansen 2002). Intense photosynthetic activity can result in pH values as high as 9 in open marine environments (Hinga 2002) and even up to 10 in coastal lagoons and fjords (Hansen 2002). Rising atmospheric CO_2 levels caused by human-induced activities such as fossil fuel burning has affected seawater carbonate chemistry. Present day surface ocean pH is approximately 0.1 units lower than preindustrial values owing to the uptake of 'anthropogenic' CO_2 into the ocean and its subsequent dissociation resulting in an increase of the H^+ concentration. By the end of this century, it is expected that the seawater pH will have dropped by 0.4 units relative to preindustrial values (Wolf-Gladrow et al. 1999, Intergovernmental Panel on Climate Change 2007). In view of this ocean acidification as well as variations in pH during blooms, the role of inorganic carbon (C_i) acquisition has received increasing attention in phytoplankton ecology and physiology.

The enzyme ribulose-1,5-bisphosphate carboxylase/oxygenase (RubisCO) fixes CO_2 into organic carbon compounds. Owing to the poor affinity of RubisCO for CO_2 (K_M of 20–70 μmol l^{-1} for eukaryotic phytoplankton, Badger et al. 1998), phytoplankton cells employ carbon-concentrating mechanisms (CCMs) to increase the CO_2 concentration at the catalytic site of this enzyme. The operation of a CCM in phytoplankton cells significantly increases the efficiency of carbon fixation, thus reported apparent half-saturation concentrations ($K_{1/2}$) values for CO_2 in microalgae are <1–8 μmol l^{-1} (Raven and Johnston 1991).

Modes of CCMs have been found to vary in terms of efficiency as well as regulation between taxonomically different groups of phytoplankton (Giordano et al. 2005). This relates to the extent to which either CO_2 or HCO_3^-, or both carbon sources, are actively transported across the plasmalemma, as well as to the presence and location of carbonic anhydrase (CA). This enzyme accelerates the otherwise slow rate of conversion between HCO_3^- and CO_2. Extracellular carbonic anhydrase (eCA) activity has been suggested to be involved in HCO_3^- utilization by converting HCO_3^- to CO_2, which is subsequently taken up by cells (Sültemeyer 1998, Elzenga et al. 2000). The physiological role of intracellular carbonic anhydrase (iCA) is still not fully understood, but it is possibly involved in different processes (Badger 2003, Badger and Price 1994, Sültemeyer 1998). Another important, but often neglected, component of a CCM is the capacity of the cell to reduce the loss of accumulated C_i by minimizing the CO_2 efflux through the cell membrane (Raven and Lucas 1985, Rost et al. 2006a, 2006b).

CCMs contribute to the competitive fitness of phytoplankton species, especially under changing pH levels. While bloom-forming diatom species operate an efficient and regulated CCM that allows maintenance of high growth rates even under elevated pH (Rost et al. 2003), slow-growing diatom species may not be able to compensate for decreasing CO_2 concentrations under these conditions. Previous studies indicate that diatoms possess highly regulated and efficient CCMs with respect to changes in CO_2 supply (Burkhardt et al. 2001, Rost et al. 2003). However, whether these are general characteristics of diatoms have yet to be rigorously tested.

Some diatom species produce the neurotoxic amino acid, domoic acid (DA). Toxic diatoms cause ecological and economic problems because of the accumulation of DA in the marine food web. Understanding toxin production is complicated because both toxic and non-toxic strains of the same species co-exist, and it is currently not clear what induces DA production (Bates et al. 1998). Lundholm et al. (2004) suggested that elevated pH-triggers DA production in different strains of *Pseudo-nitzschia*. The physiological response of toxic diatoms to changes in pH is still poorly known, and to date, no study has characterized the CCMs of toxic diatoms. Furthermore, it has not yet been investigated whether the increase of intracellular content of DA is dependent on the pH-dependent changes in carbon acquisition.

The aim of the present study was to investigate the effect of pH on C_i acquisition as well as on toxin production in three marine diatom species. Cellular uptake of CO_2 and HCO_3^- during steady-state photosynthesis of the two potentially toxic species *Pseudo-nitzschia multiseries* (a bloom-forming cosmopolitan species) and *Nitzschia navis-varingica* (which occurs in coastal marine areas and in marine ponds) as well as the non-toxic *Stellarima stellaris* (a widely distributed species) was estimated by membrane inlet mass spectrometric (MIMS) measurements. This approach was used to determine substrate preferences for CO_2 and HCO_3^- as well as possible shifts in carbon source and cellular leakage (CO_2 efflux/gross C_i uptake) with changing pH. To further characterize the CCM of each species, measurements of iCA and eCA activities were performed by monitoring ^{18}O exchange from doubly labelled $^{13}C^{18}O_2$.

Materials and methods

Culture and experimental conditions

Stellarima stellaris (isolate from the Sound, Denmark), *N. navis-varingica* (VHL987) and *P. multiseries* (OKPm013-2) were grown in dilute batch cultures in sterile-filtered (0.2 μm) unbuffered seawater, enriched with nutrients, trace metals and vitamins according to f/2 medium (Guillard and Ryther 1962). Silicate was added to a concentration of 317 μmol l^{-1}. Experiments were carried out using a light:dark cycle of 16:8 h at a constant temperature of 15°C. A photon flux density of 200 μmol photons m^{-2} s^{-1} was applied using daylight fluorescence lamps that provided a spectrum similar to that of sunlight. The applied photon flux density ensured that neither growth nor production of DA was light limited (Bates et al. 1998). Each treatment was incubated in triplicate in sterile 2.4-l borosilicate bottles. Gentle rotation of the culture flasks five times a day ensured that the cells were kept in suspension.

The medium used for the experiments was adjusted by addition of HCl or NaOH to low pH (7.9) and high pH (8.4 for *S. stellaris* and *P. multiseries*, and 8.9 for *N. navis-varingica*) on the National Bureau of Standards (NBS) scale. This corresponds to CO_2 concentrations of 31, 9.2 and 2.2 μmol kg^{-1}, respectively (Table 1). pH was measured using a pH/ion meter (model pMX 3000/pH; WTW, Weilheim, Germany) that was calibrated (two-point calibration) on a daily basis. Daily or twice-daily dilutions with fresh media ensured that the pH level remained constant (±0.05 units) and that the cells stayed in the mid-exponential growth phase. High pH levels were selected based on the upper pH limits observed in the selected species, ensuring that growth rates were not affected by the pH levels chosen. Growth rates were about 0.70 day^{-1} in *S. stellaris*, 0.95 day^{-1} in *P. multiseries* and 0.59 day^{-1} in *N. navis-varingica*. Cell concentrations ranged between 500 and 3000 cells ml^{-1} for the three species.

Determination of seawater carbonate chemistry

Alkalinity samples were taken from the filtrate (Whatman GFF filter; approximately 0.6 μm) and stored in 300-ml borosilicate flasks at 4°C and measured in triplicate by potentiometric titration with an average precision of 8 μEq kg^{-1} (Brewer et al. 1986). Total alkalinity was calculated from linear Gran Plots (Gran 1952). DIC samples were sterile-filtered (0.2 μm) and stored in 13-ml borosilicate flasks free of air bubbles at 4°C until they were measured with a total carbon analyzer (Shimadzu TOC-5050A 's-Hertogenbosch, The Netherlands) with an average precision of 17 μmol kg^{-1} in triplicate.

The carbonate system was calculated from alkalinity, DIC, silicate, phosphate, temperature and salinity using the CO2Sys program (Lewis and Wallace 1998). Equilibrium constants of Mehrbach et al. (1973) refitted by Dickson and Millero (1987) were used. The carbonate chemistry was kept constant over the duration of the experiment (Table 1).

Table 1. Parameters of the seawater carbonate system were calculated from DIC, pH, silicate, phosphate, temperature and salinity using the CO2Sys program (Lewis and Wallace 1998). Errors denote ± SD (n = 3).

pH (NBS)	TA (μEq kg^{-1})	DIC (μmol kg^{-1})	CO_2 (μmol kg^{-1})	pCO_2 (Pa)
7.9 (±0.05)	2351 ± 82	2213 ± 80	31 ± 1.1	*82.8 ± 3.0*
8.4 (±0.05)	2651 ± 94	2240 ± 84	9.2 ± 0.3	*24.6 ± 0.9*
8.9 (±0.05)	*3115 ± 78*	*2171 ± 60*	*2.2 ± 0.1*	6.0 ± 0.2

Sampling

After acclimation for at least 7 days, cells were harvested by gentle filtration over an 8-μm membrane filter (Isopore; Millipore, Schwalbach/Ts., Germany). Subsequently, the cells were washed with CO_2-free f/2 medium buffered with 50 mmol l^{-1} HEPES (pH 8.0). The samples were then used for determination of carbon (C_i) fluxes and CA activities with the MIMS. Samples for determination of Chl *a* concentration were taken after the measurements and stored at −80°C. Chl *a* was subsequently extracted in 10 ml acetone (overnight in darkness at 4°C) and determined with a Turner Designs Fluorometer.

Determination of CA activity

Activity of eCA and iCA was determined by measuring the loss of ^{18}O from doubly labelled $^{13}C^{18}O_2$ to water caused by the interconversion of CO_2 and HCO_3^- (Silverman 1982). The determination of CA activity was performed with a sector field multicollector mass spectrometer (Isoprime; GV Instruments, Manchester, UK) through a gas-permeable polytetrafluoroethylene membrane (PTFE, 0.01 mm) inlet system. The reaction sequence of ^{18}O loss from initial $^{13}C^{18}O^{18}O$ (m/z = 49), through the intermediate $^{13}C^{18}O^{16}O$ (m/z = 47) to the final isotopomer $^{13}C^{16}O^{16}O$ (m/z = 45) was recorded continuously. The ^{18}O enrichment was calculated as:

$$^{18}O\ \log(\text{enrichment}) = \log\frac{(^{13}C^{18}O_2)\times 100}{^{13}CO_2} = \log\frac{(49)\times 100}{45+47+49} \qquad (1)$$

CA measurements were performed in 8 ml f/2 medium buffered with 50 mmol l^{-1} HEPES (pH 8.0) at 15°C. To avoid interference with light-dependent C_i uptake by the cells, all measurements were carried out in the dark. When chemical equilibrium was reached after injection of 1 mmol l^{-1} $NaH^{13}C^{18}O$, the uncatalysed ^{18}O loss was monitored for about 8 min prior to the addition of cells. eCA activity was calculated from the increasing rate of ^{18}O depletion after addition of the cells (slope S_2) in comparison with the uncatalysed reaction (slope S_1) and normalized on a Chl *a* basis (Badger and Price 1989):

$$U = \frac{(S_2 - S_1)\times 100}{S_1 \times \mu g\ Chl\ a} \qquad (2)$$

iCA activity was determined in the presence of 100 μmol l^{-1} dextran-bound sulphonamide (DBS), an inhibitor of eCA. The drop in the log(enrichment) was calculated by extrapolation of S_2 back to the time of cell injection [Δ as defined by Palmqvist et al. (1994)]. Values of Δ are expressed in arbitrary units per μg Chl *a*. Chl *a* concentrations in CA assays ranged from 0.13 to 1.34 μg ml^{-1}.

Determination of net photosynthesis, CO_2 and HCO_3^- uptake

C_i fluxes were determined during steady-state photosynthesis with the same MIMS as for CA measurements. The method established by Badger et al. (1994) is based on simultaneous measurements of O_2 and CO_2 during consecutive light and dark intervals. Known amounts of C_i were added to measure photosynthesis and carbon uptake rates as a function of CO_2 and HCO_3^- or DIC concentrations. Net photosynthesis, CO_2 uptake and HCO_3^- uptake were calculated according to the equations of Badger et al. (1994). All measurements were performed in initially CO_2-free f/2 medium buffered with 50 mmol l^{-1} HEPES (pH 8.0) at 15°C. DBS was added to the cuvette to a final concentration of 100 μmol l^{-1}. Light and dark intervals during the assay lasted 6 min. The incident photon flux density was 300 μmol photons m^{-2} s^{-1}. Further details on the method and calculations are given in Badger et al. (1994) and Rost et al. (2007). Chl *a* concentrations in the assay ranged from 0.28 to 1.57 μg ml^{-1}.

Carbon isotope fractionation

Samples for particulate organic carbon (POC) were filtered onto precombusted (500°C, 12 h) GFF filters (approximately 0.6 μm) and stored in precombusted (500°C, 12 h) Petri dishes at −20°C. Prior to analysis, POC filters were treated with 200 μl HCl (0.1 N) to remove all inorganic carbon. POC and related $\delta^{13}C$ values were subsequently measured in duplicate on an EA mass spectrometer (ANCA-SL 2020; Sercon Ltd, Crewe, UK), with a precision of ±1.5 μg C and ±0.5‰, respectively. The isotopic composition is reported relative to the PeeDee belemnite standard:

$$\delta^{13}C_{Sample} = \left[\frac{(^{13}C/^{12}C)_{Sample}}{(^{13}C/^{12}C)_{PDB}} - 1\right]\times 1000 \qquad (3)$$

Isotope fractionation during POC formation (ε_p) was calculated relative to the isotopic composition of CO_2 in the medium (Freeman and Hayes 1992):

$$\varepsilon_p = \frac{\delta^{13}C_{CO_2} - \delta^{13}C_{POC}}{1 + \frac{\delta^{13}C_{POC}}{1000}} \qquad (4)$$

To determine isotopic composition of DIC ($\delta^{13}C_{DIC}$), samples were sterile filtered (0.2 μm), fixed with $HgCl_2$ (approximately 140 mg l^{-1} final concentration) and stored at 4°C. Measurements of $\delta^{13}C_{DIC}$ were performed with a Finnegan mass spectrometer (MAT 252) at a precision of $\delta^{13}C = \pm 0.05‰$. The isotopic composition of CO_2 ($\delta^{13}C_{CO2}$) was calculated from $\delta^{13}C_{DIC}$, making use of a mass balance relation (Zeebe and Wolf-Gladrow 2001):

$$\delta^{13}C_{HCO_3^-} = \frac{\delta^{13}C_{DIC}[DIC] - \left(\varepsilon_a[CO_2] + \varepsilon_b\left[CO_3^{2-}\right]\right)}{\left(1 + \varepsilon_a\times 10^{-3}\right)[CO_2] + \left[HCO_3^-\right] + \left(1 + \varepsilon_b\times 10^{-3}\right)\left[CO_3^{2-}\right]} \qquad (5)$$

$$\delta^{13}C_{CO_2} = \delta^{13}C_{HCO_3^-}\left(1 + \varepsilon_a\times 10^{-3}\right) + \varepsilon_a \qquad (6)$$

Temperature-dependent fractionation factors between CO_2 and HCO_3^- (ε_a) as well as between HCO_3^- and CO_3^{2-} (ε_b) are given by Mook (1986) and Zhang et al. (1995), respectively.

Toxin analyses

The samples for toxin analyses (600 or 1000 ml) were filtered through a 3-μm polycarbonate filter, which was never allowed to dry out. The residue on the filter was rinsed with fresh culture medium and subsequently transferred to a falcon tube and adjusted to a final volume

of 4 ml. Initial measurements on the filtered medium showed no DA (i.e. extracellular DA) in any of the treatments and consequently filtered medium was not subsequently measured. Cell counts were used for determination of toxin content per cell. Until further analysis, samples were stored at −20°C.

For preparation of the samples, 4 ml of frozen material were thawed and subsequently centrifuged at 4°C for 15 min at 2100 *g*. Because diatoms partially break during freezing and thawing cycles and cell content leaks into the medium, DA had to be determined in cell pellets and supernatant. Five hundred microlitres of the supernatant was centrifuged (Eppendorf 5415 R; Eppendorf, Hamburg, Germany) for 30 s at 800 *g* through a spin filter (pore size 0.45 μm, Millipore-Ultrafree, Eschborn, Germany) and frozen at −20°C until LC-MS/MS analysis for measurement of DA in the cell-free fraction. Cell pellets were resuspended in 0.5 ml water–methanol (1:1 v/v), transferred to FastPrep tubes containing 0.9 g of lysing matrix D (Thermo Savant, Illkirch, France) and subsequently homogenized by reciprocal shaking at maximum speed for 45 s in a Bio101 FastPrep instrument (Thermo Savant). After homogenization, samples were centrifuged at 16 100 *g* at 4°C for 15 min. Supernatants were removed and centrifuged for 30 s at 800 *g* through a spin filter and frozen at −20°C until LC-MS/MS analysis of DA in the cellular fraction.

Mass spectrometric measurements were performed on an ABI-SCIEX-4000 Q Trap, triple quadrupole mass spectrometer equipped with a TurboSpray® interface coupled to an Agilent model 1100 LC. Analyses for DA were performed in triplicate. The analytical column (250 × 4.6 mm) was packed with 5 μm Luna C18 (Phenomenex, Aschaffenburg, Germany) and maintained at 25°C. The flow rate was 1.0 ml min^{-1} and gradient elution was performed with two eluents, where eluent A was 2 mmol l^{-1} ammonium formate and 50 mmol l^{-1} formic acid in water and eluent B was 2 mmol l^{-1} ammonium formate and 50 mmol l^{-1} formic acid in acetonitrile/water (95:5 v/v). The gradient was as follows: 9 min column equilibration with 87% A, 2 min isocratic with 87% A, then linear gradient until 10 min to 50% A, then until 11 min return to initial conditions 87% A. Total run time was 20 min. Five microlitres of sample were injected.

Measurements were carried out in the multiple reaction monitoring (MRM) mode by selecting the following transitions for DA (precursor ion>fragment ion): m/z 312>266 (quantifier) and m/z 312>161 (qualifier). Dwell times of 150 ms were used for each transition. For these studies, the following source parameters were used – curtain gas: 25 psi, temperature: 600°C, ion-spray voltage: 5500 V, nebulizer gas: 55 psi, auxiliary gas: 70 psi, interface heater: on, and declustering potential: 66 V.

Results

Photosynthesis and C_i fluxes

During steady-state photosynthesis, CO_2 and HCO_3^- were taken up simultaneously by all species (Table 2). Maximum rates (V_{max}) and half-saturation concentrations ($K_{1/2}$) were obtained from a Michaelis–Menten fit to the data and are summarized in Table 2. The acclimation of a species to low and high pH had no effect on the V_{max} of photosynthetic O_2 evolution in the assay, i.e. V_{max} remained constant (Table 2). In comparison, *P. multiseries* exhibited the highest photosynthetic rates on a Chl *a* basis. In all investigated species, $K_{1/2}$ values for photosynthetic O_2 evolution decreased with rising pH (Table 2). Highest $K_{1/2}$ values were recorded in *S. stellaris* and lowest in *P. multiseries*. In all three species, $K_{1/2}$ (CO_2) values for photosynthesis were about one order of

Table 2. $K_{1/2}$ and V_{max} of photosynthesis, net CO_2 uptake and HCO_3^- uptake for *Stellarima stellaris*, *Pseudo-nitzschia multiseries* and *Nitzschia navis-varingica* acclimated to low and high pH. Kinetic parameters were calculated from a Michaelis–Menten fit to the combined data of several independent measurements. Values for $K_{1/2}$ and V_{max} are given in μmol l^{-1} and μmol (mg Chl *a*)$^{-1}$ h^{-1}, respectively. Error bars denote ±SD.

	Photosynthesis				Net CO_2 uptake		HCO_3^- uptake	
pH (NBS)	$K_{1/2}$ (CO_2)	V_{max} (CO_2)	$K_{1/2}$ (DIC)	V_{max} (DIC)	$K_{1/2}$ (CO_2)	V_{max} (CO_2)	$K_{1/2}$ (HCO_3^-)	V_{max} (HCO_3^-)
S. stellaris								
7.9	7.4 ± 1.7	258 ± 17	572 ± 133	258 ± 17	—	40 ± 29	329 ± 150	219 ± 23
8.4	4.0 ± 0.5	262 ± 9	304 ± 41	264 ± 10	—	8.6 ± 5.3	227 ± 34	254 ± 9
P. multiseries								
7.9	3.5 ± 0.5	363 ± 20	327 ± 57	368 ± 22	4.6 ± 0.6	175 ± 10	241 ± 49	190 ± 14
8.4	2.2 ± 0.3	354 ± 15	223 ± 39	369 ± 18	2.3 ± 0.3	148 ± 8	186 ± 63	218 ± 15
N. navis-varingica								
7.9	4.6 ± 0.7	262 ± 10	494 ± 67	261 ± 9	6.0 ± 1.0	221 ± 10	—	42 ± 4
8.9	3.1 ± 0.9	287 ± 19	301 ± 84	290 ± 18	6.6 ± 1.2	203 ± 11	—	89 ± 8

magnitude lower than the K_M (CO_2) values known for RubisCO in diatoms (approximately 30–40 μmol CO_2 l^{-1}; Badger et al. 1998).

In terms of CO_2 uptake, the $K_{1/2}$ values for *N. navis-varingica* and *P. multiseries* were generally between 4 and 7 μmol l^{-1}, only in *P. multiseries* the acclimation to high pH induced higher affinities (Table 2). The V_{max} for net CO_2 uptake for *N. navis-varingica* and *P. multiseries* ranged between 148 and 221 μmol (mg Chl a)$^{-1}$ h^{-1}. In *S. stellaris*, net CO_2 uptake was very low and hence no $K_{1/2}$ values could be estimated. Regarding the HCO_3^- uptake, $K_{1/2}$ values in *P. multiseries* and in *S. stellaris* were generally <330 μmol l^{-1} and decreased when acclimated to high pH. In *S. stellaris*, the V_{max} of HCO_3^- uptake was slightly higher than that for *P. multiseries*. For *N. navis-varingica*, the HCO_3^- uptake was low and could not be described by Michaelis–Menten kinetics.

Using the uptake kinetics obtained in the assay, the contribution of HCO_3^- uptake relative to carbon fixation for the conditions of the respective incubations was estimated (Fig. 1). The preference for HCO_3^- uptake strongly increased in *N. navis-varingica* with rising pH, while the different pH acclimations yielded similar ratios in *P. multiseries* and *S. stellaris*. With values larger than 85%, the preference for HCO_3^- is very high in *S. stellaris*, whereas *P. multiseries* reached values of approximately 55%. In *N. navis-varingica*, the contribution of HCO_3^- uptake relative to net fixation accounted for at most approximately 30% under high pH, reflecting a strong preference for CO_2.

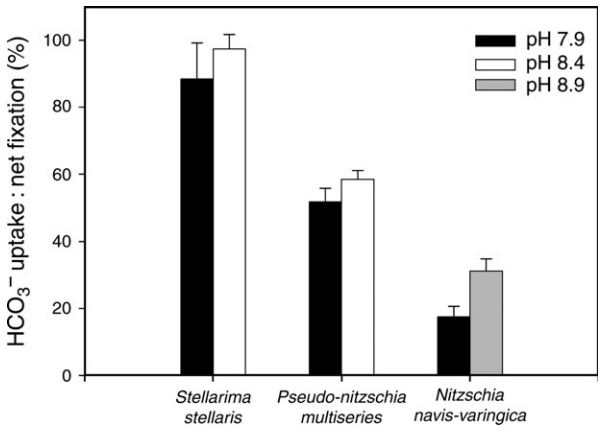

Fig. 1. Ratios of HCO_3^- uptake to net photosynthesis of cells acclimated to different pH levels. Ratios from MIMS measurements were based on the rates obtained at C_i concentrations of about 2 mmol l^{-1}.

eCA and iCA activity

Activity of eCA was high in *P. multiseries* and *S. stellaris* and increased with elevated pH (Fig. 2A). In *N. navis-varingica*, eCA activities were low and remained constant independent of the pH. The activities of iCA remained constant in all investigated species, independent of the pH of the acclimation (Fig. 2B).

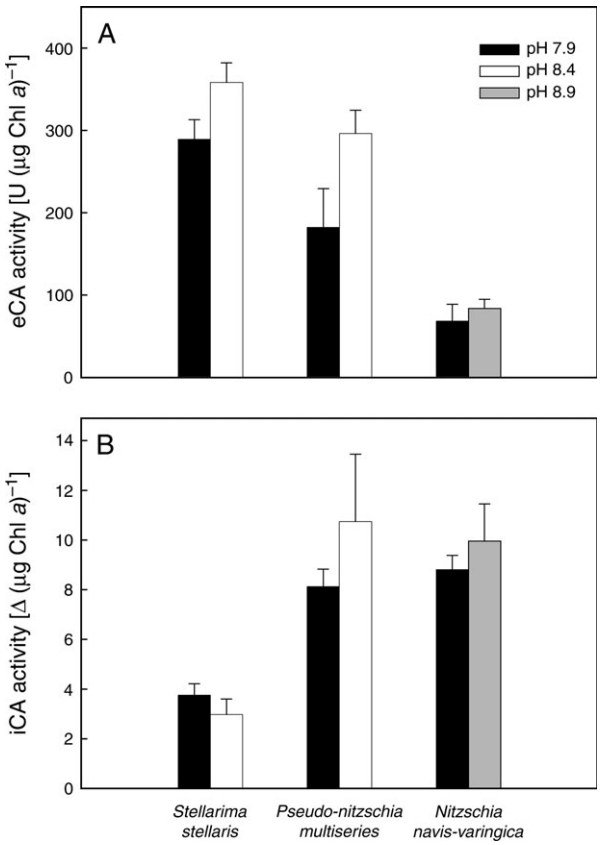

Fig. 2. Chl *a*-specific activities of (A) eCA and (B) iCA activities from cells acclimated to low and high pH. Values represent the means of triplicate incubations (±SD).

Carbon isotope fractionation and leakage

Carbon isotope fractionation decreased with rising pH in all investigated species (Fig. 3). The strongest reduction in ε_p was observed in *N. navis-varingica*, with ε_p being 9.8‰ under low pH and 3.7‰ at high pH. *S. stellaris* obtained highest fractionation values in comparison with the two other species, its ε_p ranged between 11.5 and 14.4‰.

The leakage of cells, i.e. the proportion of C_i efflux compared with gross C_i uptake, was estimated by MIMS through the CO_2 efflux recorded immediately after the light had been turned off (Badger et al. 1994). For all species, leakage was highest at the lowest CO_2 concentrations and levelled off towards higher CO_2 concentrations in the assay (Fig. 4). With increasing pH, leakage appeared to decrease mainly in *N. navis-varingica*.

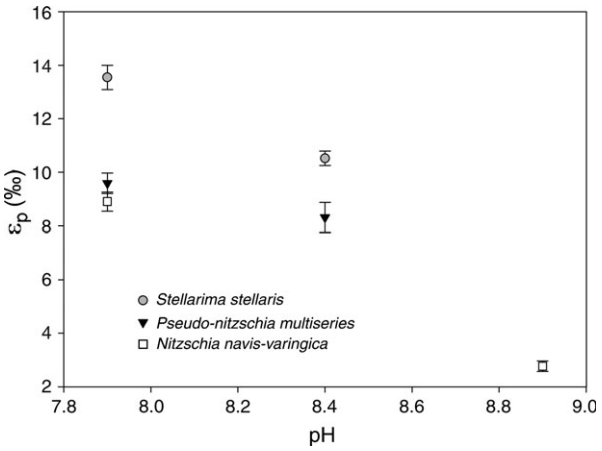

Fig. 3. Isotope fractionation (ε_p) as a function of pH, calculated from the $^{13}C_{CO2}$ and $^{13}C_{POC}$ in the respective acclimations of each species. Error bars denote ±SD (n = 3).

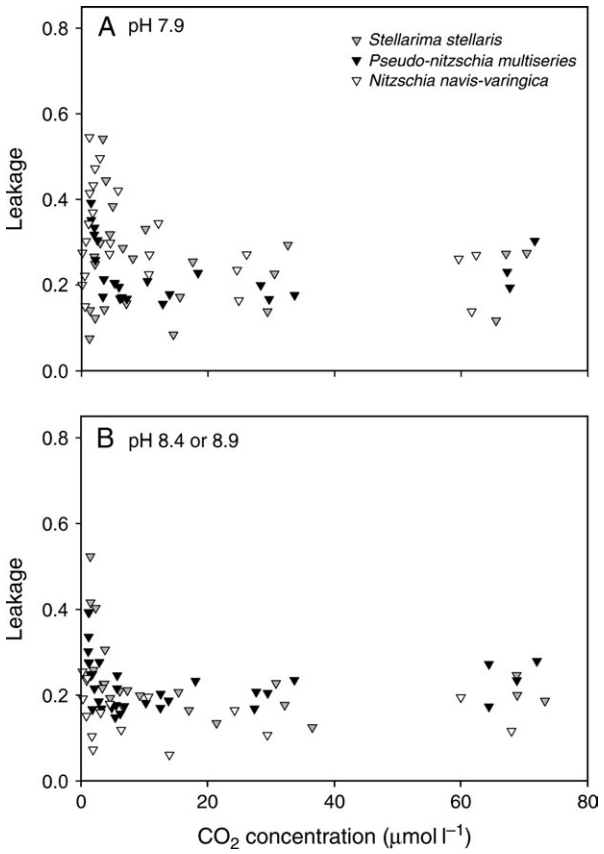

Fig. 4. Leakage of the cells, i.e. the proportion of C_i efflux relative to gross C_i uptake, as a function of the CO_2 concentration in the C_i flux assay from each species acclimated to (A) low and (B) high pH.

DA production

The content of DA per cell differed with pH, both for *P. multiseries* and for *N. navis-varingica*. Increasing pH resulted in increasing content of DA (Table 3). The differences were, however, only significant between the pH levels for *P. multiseries* (Student's *t*-test, $P < 0.01$). No DA was detected in *S. stellaris* at any of the pH levels.

Discussion

The application of MIMS techniques such as the estimation of CA activities and C_i fluxes, in combination with analyses of ^{13}C fractionation, allowed detailed characterization of the CCM in each species. Acclimations to low and high pH were performed in unbuffered seawater with low cell densities to simulate natural conditions as closely as possible. High affinities for C_i were observed in all investigated species, indicating the operation of a CCM (Table 2). All species upregulated their CCM activity when acclimated to high pH. Despite these similarities, strong species-specific differences in the modes of carbon acquisition existed.

Photosynthetic O_2 evolution

Apparent $K_{1/2}(CO_2)$ for photosynthesis lower than K_M (CO_2) of RubisCO provides evidence for the operation of a CCM (Badger et al. 1998). In our experiments, $K_{1/2}(CO_2)$ values for photosynthesis were low in all investigated species, ranging from 2.2 to 7.4 µmol CO_2 (Table 2). These values are about an order of magnitude lower than known K_M (CO_2) values for RubisCO in diatoms (31–36 µmol CO_2 l^{-1} in two strains of *Cylindrotheca* sp. and 41 µmol CO_2 l^{-1} in *Phaeodactylum tricornutum*; Badger et al. 1998), indicating that the investigated species possessed highly efficient CCMs. All three species had upregulated their carbon acquisition with decreasing CO_2 supply (Table 2). The observed affinities are comparable with previous findings obtained with MIMS techniques in marine diatoms (Burkhardt et al. 2001, Rost et al. 2003). By measuring the photosynthetic O_2 evolution upon the addition of varying C_i concentrations and assuming equilibrium concentrations for CO_2,

Table 3. The intracellular content of DA in the investigated diatoms acclimated to different pH levels. Values represent the mean of triplicates ± SD.

	Nitzschia navis-varingica		*Pseudo-nitzschia multiseries*		
pH	7.9	8.9	7.9	8.4	8.9
Intracellular toxin content (pg $cell^{-1}$)	158 ± 15	213 ± 28	1.9 ± 0.3	4.2 ± 0.4	140 ± 8

$K_{1/2}(CO_2)$ values for photosynthetic O_2 evolution have been estimated (Burns and Beardall 1987, Colman and Rotatore 1995, Mitchell and Beardall 1996). Mitchell and Beardall (1996) calculated the $K_{1/2}(CO_2)$ value to be approximately 1.09 μmol l^{-1} at pH 7.5 in the sea-ice diatom *Nitzschia frigida*. Colman and Rotatore (1995) demonstrated $K_{1/2}(CO_2)$ values of 1.44 μmol l^{-1} for *Cyclotella* sp. and 4.01 μmol l^{-1} for *P. tricornutum*. For the latter species, Burns and Beardall (1987) obtained an even lower $K_{1/2}(CO_2)$ value of 0.53 μmol CO_2 l^{-1}. In summary, the CO_2/pH-induced changes in apparent C_i affinities and the generally low $K_{1/2}(CO_2)$ for photosynthesis indicate highly efficient and regulated CCMs in the investigated species.

Carbon sources and uptake kinetics

To understand why a certain species appears to have a more or less efficient carbon acquisition, in other words different abilities to reach C_i-saturated rates in photosynthesis, the different components of the CCM must be characterized. In the present study, CO_2 and HCO_3^- rates were estimated following the method of Badger et al. (1994). This approach has the advantage that it also allows determination of carbon uptake kinetics during steady-state photosynthesis. While several studies demonstrated that simultaneous uptake of CO_2 and HCO_3^- occurs in marine diatoms (e.g. Burns and Beardall 1987, Korb et al. 1997, Rotatore et al. 1995, Tortell and Morel 2002), a finding that is consistent with our results, little information exists on uptake kinetics for individual carbon sources (e.g. Burkhardt et al. 2001, Rost et al. 2003, Rost et al. 2006a).

The efficiency of a CCM is strongly depending on the characteristics of the C_i uptake systems. Higher transport rates for CO_2 and/or HCO_3^- can be achieved in two ways: either by increasing the affinities for the respective C_i species through a higher substrate-binding capacity (e.g. Amoroso et al. 1998, Matsuda and Colman 1995, Palmqvist et al. 1994) or by an increase in the number of transporters (e.g. Burkhardt et al. 2001, Rost et al. 2003). According to our results, species responded differently to pH-induced changes in carbonate chemistry. *P. multiseries* used CO_2 and HCO_3^- in equal quantities, which did not change with pH (Fig. 1). This is the result of an increased substrate affinity of the CO_2 uptake system, which compensated for the lower CO_2 availability at high pH (Fig. 1). *N. navis-varingica* was characterized by a strong preference for CO_2 ('CO_2 user'), although the contribution of HCO_3^- uptake relative to net fixation increased with rising pH (Table 2). The latter might be because of a larger number of HCO_3^- transporters when acclimated to high pH (Table 2). *S. stellaris* showed a strong preference for HCO_3^- ('HCO_3^- user') irrespective of the acclimation pH (Fig. 1). This observation is consistent with constitutively expressed C_i transport systems (Table 2). The large differences in preference for C_i sources in the group of diatoms are in agreement with those of Burkhardt et al. (2001) who showed that *Thalassiosira weissflogii* exhibited a much higher proportion of HCO_3^- uptake relative to total C_i uptake compared with *P. tricornutum*, the latter preferring CO_2 even at the highest pH level. Rost et al. (2003) showed an increasing contribution of HCO_3^- to total C_i uptake with decreasing CO_2 concentrations as a consequence of both an increasing number of HCO_3^- transport components and the induction of high-affinity C_i uptake systems. Hence, based on our data and on previous investigations, marine diatoms appear to strongly differ in terms of their preferred C_i source and the regulation of its uptake.

CA activity and its dependence on the carbon source

The enzyme CA plays an important role in carbon acquisition by accelerating the otherwise slow interconversion of CO_2 and HCO_3^-, both inside the cell and at the cell surface. The activities of eCA strongly differed between species in our investigation (Fig. 2A), being highest with 360 U (μg Chl *a*)$^{-1}$ in *S. stellaris* and lowest with 80 U (μg Chl *a*)$^{-1}$ in *N. navis-varingica*. In other words, these values correspond to an enhancement in the interconversion between HCO_3^- and CO_2 relative to the uncatalysed rate by 360 and 80% per μg Chl *a*, respectively. These activities are within the same range as those reported in Burkhardt et al. (2001) and Rost et al. (2003) [note that activities in these studies were erroneously stated as (mg Chl *a*)$^{-1}$ instead of (μg Chl *a*)$^{-1}$]. Mitchell and Beardall (1996) used a potentiometric approach to estimate CA activities (Wilbur and Anderson 1948) in *N. frigida*. They measured low eCA activities of 0.123 (μg Chl *a*)$^{-1}$ Wilbur–Anderson units, which corresponds to an enhancement in the rate constants of only approximately 12% per μg Chl *a* relative to the uncatalysed rate. According to our results and those of Mitchell and Beardall (1996), we conclude that eCA plays only a minor role in carbon acquisition in the genus *Nitzschia*.

The induction of eCA activity was found to be pH dependent both in laboratory culture experiments (Sültemeyer 1998, Burkhardt et al. 2001, Badger 2003, Rost et al. 2003) and in field experiments (Berman-Frank et al. 1994, Tortell et al. 2006). It is a common notion that eCA is involved in *indirect* HCO_3^- utilization by converting HCO_3^- to CO_2, which could then be actively

transported through the plasma membrane and subsequently used for photosynthesis (Elzenga et al. 2000, Sültemeyer 1998, Tortell et al. 2006). It should be emphasized here that high eCA activities would provide an advantage especially for large cells because large phytoplankton are more prone to CO_2 shortage in their diffusive boundary layer (Wolf-Gladrow and Riebesell 1997). Such a function of eCA in supplying CO_2 from the large HCO_3^- pool would, however, not apply at high pH because the equilibrium is strongly on the side of HCO_3^-.

In the present study, the investigated diatoms are rather large with volumes of 1030 μm^3 for *P. multiseries*, 4350 μm^3 for *N. navis-varingica* and 7720 μm^3 for *S. stellaris*. Although the highest level of eCA activity was found under high pH in the largest diatom species *S. stellaris* (Fig. 2A), this species showed a strong preference for HCO_3^- uptake and *not* for CO_2 uptake (Fig. 1). Hence, the common notion that eCA supplies CO_2 to the uptake systems is called into question in this situation. Here, we propose a mechanism that acts as a C_i-recycling mechanism at high pH in 'HCO_3^- user' (Fig. 5A), i.e. CO_2 leaking out of the cell would be converted by eCA to HCO_3^- and subsequently taken up through HCO_3^- transporters. Such a mechanism would be most efficient when the CA-mediated conversion is localized to the periplasmic space, i.e. in close vicinity to the HCO_3^- transporter. It can be hypothesized that the HCO_3^- transport process is linked to the eCA activity. Support for this idea comes from red blood cells where a plasma membrance HCO_3^-/Cl^- transporter physically binds a CAII protein (Sterling et al. 2001). In contrast to 'HCO_3^- users' like *S. stellaris*, the CO_2 user *N. navis-varingica* was characterized by low levels of eCA even under high pH (Fig. 2A). Because of rather low eCA activities, CO_2 leaking out of the cell is prevented from fast conversion to HCO_3^-, and a disequilibrium at the cell surface persists (Fig. 5B). Elevated CO_2 in turn increases the probability that the CO_2 is transported back into the cell through CO_2 transport systems. We therefore suggest that low or absent eCA activities in CO_2 users allow for efficient CO_2 recycling at high pH (Fig. 5B).

The proposed C_i-recycling mechanisms for CO_2 and HCO_3^- users at elevated pH would explain results from previous studies, i.e. the correlation of high eCA activity and HCO_3^- uptake and the lack of eCA in CO_2 users. Burkhardt et al. (2001) observed high eCA activities and high HCO_3^- uptake rates in *T. weissflogii*, while *P. tricornutum* showed a preference for CO_2 and eCA activities were low. *Skeletonema costatum* combined both extremes, i.e. high eCA activities and predominant HCO_3^- uptake under high pH, whereas eCA was lacking at low pH accompanied by a strong preference for CO_2 (Rost et al. 2003). We consequently conclude, based on our data and that of previous investigations, that the presence or absence of eCA allows for a more efficient C_i recycling in 'HCO_3^-' and 'CO_2' users, respectively.

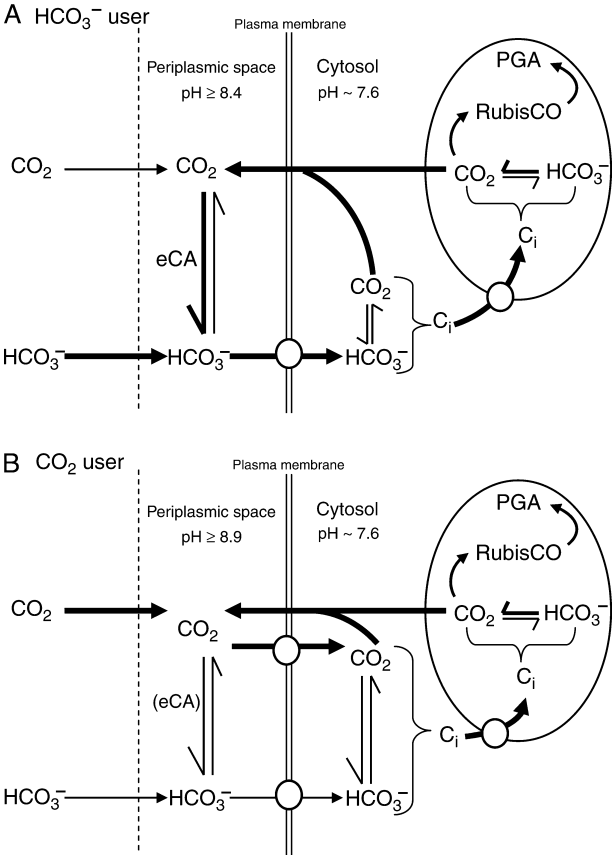

Fig. 5. Model of the C_i-recycling mechanism. The cytosolic pH is assumed to be approximately 7.6 (Burns and Beardall 1987, Colman and Rotatore 1995) while the pH in the periplasmic space is assumed to be elevated with respect to the pH in the bulk media. (A) In 'HCO_3^- user' as *Stellarima stellaris*, the CO_2 leaking out of the cell would be converted by eCA to HCO_3^- and subsequently taken up through HCO_3^- transporters. (B) In 'CO_2 user' as *Nitzschia navis-varingica*, CO_2 is prevented from conversion to HCO_3^- and a disequilibrium in the boundary layer persists. As the CO_2 leaking out of the cell remains in the form of CO_2 at the cell surface, the probability increases that the CO_2 is transported back into the cell through CO_2 transport systems. Note that in the chloroplast CO_2 is being fixed by RubisCO to produced PGA and sugars.

The physiological role of internally located CA (iCA) is still poorly understood (Sültemeyer 1998) because of the occurrence of multiple CA forms in the cytosol, chloroplast and mitochondria, but there is evidence that iCAs are important components of the CCM (Badger and Price 1994, Sültemeyer 1998, Badger 2003). Prior to our discussion on iCA activities, we would like to point out some of the assumptions underlying the applied approach to estimate iCA activities (Palmqvist et al. 1994). First, it should be noted that the results shown in Fig. 2B do not

differentiate between the multiple CA forms and their location. Estimates on iCA activities are also dependent on the rate of diffusive influx of ^{18}O-labelled CO_2 and thus can be altered by the diffusive properties of the cell membrane, intracellular pH and cell size and shape. In addition, Rost et al. (2003) showed that assessing iCA activities without applying inhibitors for eCA affects the absolute estimates. Because of these uncertainties, the following species comparison should be interpreted with caution.

High iCA levels were expressed in the CO_2 user *N. navis-varingica*, while lowest activities were found in the HCO_3^- user *S. stellaris* (Fig. 2B). Provided that iCA observed in the latter species is predominantly reflecting CA located in the cytosol, the low activity would prevent the taken up HCO_3^- from being converted to CO_2 and hence it would remain in the form of HCO_3^- for which cell membranes are highly impermeable. In contrast, high iCA levels in the CO_2 user *N. navis-varingica* enhance the conversion of CO_2 to HCO_3^- in the cytosol. This interpretation of our data is supported by the observation of Price and Badger (1989) that the absence of cytosolic CA activity in *Synechococcus*, a HCO_3^- user, is crucial for minimizing CO_2 leakage. Consequently, the expression of human CA in the cytosol led to loss of the ability to accumulate internal C_i. All data together, we propose that the presence or absence of iCA functions to minimize the loss of CO_2. Evidence for such a CO_2-trapping mechanism is supported by a model study at the level of the chloroplast (Thoms et al. 2001). Further research in marine diatoms is needed to evaluate the potential role of iCA acting as a CO_2-trapping mechanism.

Carbon isotope fractionation and leakage

Carbon isotope fractionation can provide information on modes of carbon uptake in marine phytoplankton (Raven and Johnston 1991, Rost et al. 2002). The interpretation of such data often remains complicated because of a lack of knowledge on processes involved in fractionation. In the present study, the information on the CCM derived by MIMS techniques permits a more thorough analysis of carbon isotope fractionation data. According to the model proposed by Sharkey and Berry (1985), variations in ε_p are mainly determined by the carbon source taken up and the so-called leakage (L), defined as the ratio of CO_2 efflux to the total C_i uptake:

$$\varepsilon_p = a \times \varepsilon_S + L \times \varepsilon_f \qquad (7)$$

In this equation, *a* represents the fractional contribution of HCO_3^- to total C_i uptake and ε_s is the equilibrium discrimination between CO_2 and HCO_3^- (approximately $-10‰$). The fractionation of the carbon-fixing enzyme RubisCO (ε_f) is assumed to be 29‰. As HCO_3^- is about 10‰ enriched in ^{13}C compared with CO_2 (Zeebe and Wolf-Gladrow 2001), an increasing proportion of HCO_3^- uptake diminishes ε_p, which is defined relative to CO_2 as the carbon source. If there is no change in carbon source, ε_p decreases with decreasing leakage. Based on these considerations, carbon isotope data may provide information on the mode of carbon acquisition and vice versa. In terms of information on the carbon source, only extreme ε_p values allow precluding one carbon source. If ε_p is lower than 0‰, CO_2 can be excluded as the only carbon source, while ε_p values higher than 20‰ rule out HCO_3^- as the only carbon source.

In our study, ε_p values were found to be in between these extreme values, being consistent with both CO_2 and HCO_3^- uptake. Moreover, ε_p decreases with increasing pH in all species (Fig. 3). This trend is consistent with results obtained by Burkhardt et al. (1999a, 1999b, 2001), who found ε_p to increase with decreasing pH in six marine diatom species. Reasons for this trend will be discussed in the following sections. According to Eqn 7, a higher contribution of HCO_3^- uptake to net fixation will reduce ε_p. The 15% higher HCO_3^- contribution at high pH observed in *N. navis-varingica* (Fig. 1) would explain only 1.5‰ lower ε_p values, far less than the observed 6‰ difference between pH treatments. In the other two species, the HCO_3^- contribution did not change between the pH levels (Fig. 1). Consequently, most of the variation in ε_p observed in all investigated species has to result from changes in leakage. Taking the measured ε_P (Fig. 3) as well as the estimates of *a* obtained through the C_i flux assays, leakage was calculated according to Eqn 7 (Fig. 6). The calculated values decreased with increasing pH in all species, but between species, large differences were found. Highest values were calculated for *S. stellaris* (0.67 and 0.73 at high and low pH, respectively) and lowest values for *N. navis-varingica* (0.22 and 0.39 at high and low pH, respectively).

Because the calculated leakage is based on the assumption that the cell consists of a single compartment, an assumption obviously not matching the real structure of eukaryotic cells, it should be pointed out that the calculated leakage may only serve as an approximation of the maximal possible leakage. Any internal C_i cycling at the level of the chloroplast will decrease the leakage and subsequently ε_p (Schulz et al. 2007). Another shortcoming of the model by Sharkey and Berry (1985) is the assumption of a complete equilibrium of the carbonate system. According to Raven (1997), HCO_3^- is considered as the carbon source that enters

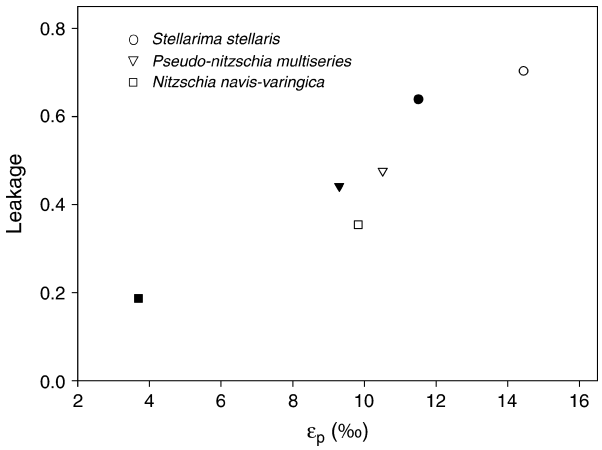

Fig. 6. Leakage of the cells as a function of ε_p, calculated according to Sharkey and Berry (1985). Closed and open symbols represent high and low pH, respectively.

the acidic thylakoid lumen (pH = 5). For such a low pH, the spontaneous rate of HCO_3^- to CO_2 conversion is sufficient to explain the observed C-fixation by RubisCO (Thoms et al. 2001). Subsequently, CA activity inside the thylakoid lumen is not necessary as previously suggested by Raven (1997). Considering that the uncatalysed conversion of HCO_3^- to CO_2 accounts for 22‰ (O'Leary et al. 1992), the CO_2 supply at the site of RubisCO in the thylakoid lumen would be isotopically lighter and hence shift ε_p to higher values. However, the latter assumes that there is no back conversion of CO_2 to HCO_3^- in the lumen, i.e. a complete non-equilibrium exists. In order to estimate the actual state of the carbonate system in the lumen, a detailed calculation is essential (Thoms et al. in preparation).

We also employed the MIMS to get estimates on leakage following the approach by Badger et al. (1994). Leakage was relatively low in all three species and diminished only in *N. navis-varingica* with increasing pH (Fig. 4). It should be noted here that these calculations are based on several assumptions, for instance, that the rate of diffusive CO_2 efflux is well represented during the first seconds of the subsequent dark phase. This approach may underestimate the real C_i efflux because of re-fixation of CO_2 by RubisCO in the dark (Badger et al. 1994, Rost et al. 2006b). Furthermore, a prerequisite for the application of this approach is the absence of eCA activity, which we ensured by the addition the eCA inhibitor DBS. Because eCA might act as a C_i-recycling mechanism, the inhibition of this enzyme may have an effect on the CO_2 efflux estimates. This underlines that new approaches are required to obtain better estimates on the important aspect of leakage.

Relationship between pH, carbon acquisition and DA production

It has been reported that higher DA production occurred at elevated pH in different strains of *P. multiseries* (Lundholm et al. 2004). To explain this effect, it has been proposed that toxin production could be induced by carbon limitation with increasing pH (Lundholm et al. 2004). In our experiments, as expected, DA was produced in the two potentially toxic species *P. multiseries* and *N. navis-varingica*, while no production was found in the non-toxic species *S. stellaris*. The content of DA increased significantly in both toxic species with increasing pH (Table 3) but was most pronounced for *P. multiseries*, where the increase in cellular DA content was more than 70-fold. This finding confirms the observation by Lundholm et al. (2004) that increasing pH induces higher DA levels. With respect to rather low values of $K_{1/2}$ for photosynthesis in *P. multiseries* and *N. navis-varingica* (Table 2), significant DIC limitation is not indicated even under high pH. Consequently, the suggested relationship between DA and carbon acquisition/C_i limitation cannot be confirmed. It is hence likely that pH triggers the DA production in another way than by altering the carbonate chemistry. As such, external pH could affect internal pH, which in turn could alter many processes that are not associated to carbon acquisition or limitation (Hansen et al. 2007). The importance of pH should therefore be considered in future monitoring programmes for harmful phytoplankton species.

Ecological implications and conclusions

In view of the ongoing acidification of the oceans (Wolf-Gladrow et al. 1999, Orr et al. 2005) as well as elevated pH during blooms (Hansen 2002), the observed differences in CCM efficiency and regulation of the investigated diatoms may play an important role for the dominance of certain diatom species (Tortell et al. 2002, Rost et al. 2003). It is a common notion that species being able to use the large HCO_3^- pool may have a competitive advantage over those that rely on CO_2 and thus may be less sensitive to variations in pH (Hansen 2002, Korb et al. 1997, Nimer et al. 1997, Tortell and Morel 2002). Consequently, elevated pH should especially favour species that prefer HCO_3^- as their carbon source. However, the pH limit for growth for the predominant HCO_3^- user *S. stellaris* was already attained at pH 8.8 (Lundholm, unpublished data) although most of the DIC was present in the form of its preferred carbon source. *S. costatum* showed a strong preference for HCO_3^- under high pH (Rost et al. 2003), but growth was already affected above pH 8.5 (Schmidt and Hansen

2001). In contrast, the CO_2 user *N. navis-varingica* grew up to pH values of 10 (Lundholm, unpublished data, Kotaki et al. 2000). Similarly, the CO_2 user *P. tricornutum* (Burkhardt et al. 2001) can maintain growth up to pH 10 (Goldman et al. 1982, Humphrey 1975). Such high pH limits for growth in CO_2 users call into question the common notion that 'HCO_3^- users' have a competitive advantage over CO_2 users. According to our data and those of previous investigations, 'HCO_3^- users' are as sensitive as CO_2 users with regard to their pH/CO_2 dependence of growth. This finding is surprising because the CO_2 availability is strongly reduced at high pH and thus CO_2 users should be *more* prone to elevated pH. The underlying mechanisms are unclear but may point to species-specific differences in leakage (Rost et al. 2006b) as well as direct effects of pH (Hansen et al. 2007). The latter could have impact on the ion balance of the cell and hence transporter functioning and energy requirements.

Bloom-forming phytoplankton species should be especially dependent on an efficient and regulated CCM as they maintain high growth rates even under bloom conditions when pH rises because of photosynthetic carbon consumption (e.g. Elzenga et al. 2000, Rost et al. 2003). The bloom-forming species *P. multiseries* obtained approximately 30% higher V_{max} of photosynthetic O_2 evolution compared with the non-bloom-forming species (Table 2). Considering that CO_2 concentrations may be as low as 5 μmol l^{-1} towards the end of a bloom, the high C_i affinity observed in bloom-forming species like *P. multiseries* directly translates to higher rates of carbon fixation. Moreover, bloom-forming diatom species tend to be more flexible in the use of different carbon sources (Fig. 1). These abilities may provide a competitive advantage, especially under changing conditions as they occur during a bloom. According to our results, the diatoms as group differ strongly in their mode of carbon acquisition and hence generalizations cannot be made.

References

Amoroso G, Sültemeyer D, Thyssen C, Fock HP (1998) Uptake of HCO_3^- and CO_2 in cells and chloroplasts from the microalgae *Chlamydomonas reinhardtii* and *Dunaliella tertiolecta*. Plant Physiol 116: 193–201

Badger MR, Price GD (1989) Carbonic anhydrase activity associated with the cyanobacterium *Synechococcus* PCC7942. Plant Physiol 89: 51–60

Badger MR, Price GD (1994) The role of carbonic anhydrase in photosynthesis. Annu Rev Plant Physiol Plant Mol Biol 45: 369–392

Badger MR, Palmqvist K, Yu J-W (1994) Measurement of CO_2 and HCO_3^- fluxes in cyanobacteria and microalgae during steady-state photosynthesis. Physiol Plant 90: 529–536

Badger MR, Andrews TJ, Whitney SM, Ludwig M, Yellowlees DC, Leggat W, Price GD (1998) The diversity and coevolution of Rubisco, plastids, pyrenoids, and chloroplast-based CO_2-concentrating mechanisms in algae. Can J Bot 76: 1052–1071

Badger MR (2003) The role of carbonic anhydrases in photosynthetic CO_2 concentrating mechanisms. Photosynth Res 77: 83–94

Bates SS, Garrison DL, Horner RA (1998) Bloom dynamics and physiology of domoic-acid producing *Pseudo-nitzschia* species. In: Anderson DM, Cembella AD, Hallegraeff GM (eds) Physiological Ecology of Harmful Algal Blooms. Springer, Berlin, pp 267–292

Berman-Frank I, Zohary T, Erez J, Dubinsky Z (1994) CO_2 availability, carbonic anhydrase and the annual dinoflagellate bloom in Lake Kinneret. Limnol Oceanogr 39: 1822–1834

Brewer PG, Bradshow AL, Williams RT (1986) Measurement of total carbon dioxide and alkalinity in the North Atlantic Ocean in 1981. In: Trabalka JR, Reichle DE (eds) The Changing Carbon Cycle – A Global Analysis. Springer, New York, pp 358–381

Burkhardt S, Riebesell U, Zondervan I (1999a) Effects of growth rate, CO_2 concentration, cell size on the stable carbon isotope fractionation in marine phytoplankton. Geochim Cosmochim Acta 63: 3729–3741

Burkhardt S, Riebesell U, Zondervan I (1999b) Stable carbon isotope fractionation by marine phytoplankton in response to daylength, growth rate, and CO_2 availability. Mar Ecol Prog Ser 184: 31–41

Burkhardt S, Amoroso G, Riebesell U, Sültemeyer D (2001) CO_2 and HCO_3^- uptake in marine diatoms acclimated to different CO_2 concentrations. Limnol Oceanogr 46: 1378–1391

Burns BD, Beardall J (1987) Utilization of inorganic carbon acquisition by marine microalgae. J Exp Mar Bio Ecol 107: 75–86

Colman B, Rotatore C (1995) Photosynthetic inorganic carbon uptake and accumulation in two marine diatoms. Plant Cell Environ 18: 919–924

Dickson AG, Millero FJ (1987) A comparison of the equilibrium constants for the dissociation of carbonic acid in seawater media. Deep Sea Res 34: 1733–1743

Elzenga JTM, Prins HBA, Stefels J (2000) The role of extracellular carbonic anhydrase activity in inorganic carbon utilization of *Phaeocystis globosa* (Prymnesiophyceae): a comparison with other marine algae using the isotope disequilibrium technique. Limnol Oceanogr 45: 372–380

Freeman KH, Hayes JM (1992) Fractionation of carbon isotopes by phytoplankton and estimates of ancient CO_2 levels. Global Biogeochem Cycles 6: 185–198

Giordano M, Beardall J, Raven JA (2005) CO_2 concentrating mechanisms in algae: mechanisms, environmental

modulation, and evolution. Annu Rev Plant Biol 56: 99–131
Goldman JC, Riley CB, Dennett MR (1982) The effect of pH in intensive microalgal cultures. II. Species competition. J Exp Mar Biol Ecol 57: 15–24
Gran G (1952) Determinations of the equivalence point in potentiometric titrations of seawater with hydrochloric acid. Oceanol Acta 5: 209–218
Guillard RRL, Ryther JH (1962) Studies of marine planktonic diatoms. Can J Microbiol 8: 229–239
Hansen PJ (2002) Effect of high pH on the growth and survival of marine phytoplankton: implications for species succession. Aquat Microb Ecol 28: 279–288
Hansen PJ, Lundholm N, Rost B (2007) Growth limitation in marine red-tide dinoflagellates: effects of pH versus inorganic carbon availability. Mar Ecol Prog Ser 334: 63–71
Hinga KR (2002) Effects of pH on coastal marine phytoplankton. Mar Ecol Prog Ser 238: 281–300
Humphrey GF (1975) The photosynthesis: respiration ratio of some unicellular marine algae. J Exp Mar Biol Ecol 18: 111–119
Intergovernmental Panel on Climate Change (2007) Working Group I Report ''The Physical Science Basis''. Available at http://ipcc-wg1.ucar.edu/wg1/wg1-report.html
Korb RE, Saville PJ, Johnston AM, Raven JA (1997) Sources for inorganic carbon for photosynthesis by three marine species of marine diatom. J Phycol 33: 433–440
Kotaki Y, Koike K, Yoshida M, Thuoc CV, Huyen NTM, Hoi NC, Fukoyo Y, Kodama M (2000) Domoic acid production in *Nitzschia* sp. (Bacillariophyceae) isolated from a shrimp-culture pond in Do Son, Vietnam. J Phycol 36: 1057–1060
Lewis E, Wallace DWR (1998) Program Developed for CO_2 System Calculations. ORNL/CDIAC-105. Carbon Dioxide Information Analysis Center. Oak Ridge National Laboratory, U.S. Department of Energy
Lundholm N, Hansen PJ, Kotaki Y (2004) Effect of pH on growth and domoic acid production by potentially toxic diatoms of the genera *Pseudo-nitzschia* and *Nitzschia*. Mar Ecol Prog Ser 273: 1–15
Matsuda Y, Colman B (1995) Induction of CO_2 and bicarbonate transport in the green alga *Chlorella ellipsoidea*. I. Time course of induction of the two systems. Plant Physiol 108: 247–252
Mehrbach C, Culberson C, Hawley J, Pytkovicz R (1973) Measurement of the apparent dissociation constants of carbonic acid in seawater at atmospheric pressure. Limnol Oceanogr 18: 897–907
Mitchell C, Beardall J (1996) Inorganic carbon uptake by an Antarctic sea-ice diatom, *Nitzschia frigida*. Polar Biol 16: 95–99
Mook WG (1986) ^{13}C in atmospheric CO_2. Neth J Sea Res 20: 211–223
Nelson DM, Tréguer P, Brzezinski MA, Leynaert A, Quéginer B (1995) Production and dissolution of biogenic silica in the ocean: Revised global estimates, comparison with regional data and relationship to biogenic sedimentation. Global Biogeochem Cycles 9: 359–372
Nimer, NA, Iglesias-Rodriguez MD, Merrett MJ (1997) Bicarbonate utilization by marine phytoplankton species. J Phycol 33: 625–631
O'Leary MH, Madhavan S, Paneth P (1992) Physical and chemical basis of carbon isotope fractionation in plants. Plant Cell Environ 15: 1099–1104
Orr JC, Fabry VJ, Aumont O, Bopp L, Doney SC, Feely RA, Gnanadesikan A, Gruber N, Ishida A, Joos F, Key RM, Lindsay K, Maier-Reimer E, Matear R, Monfray P, Mouchet A, Najjar RG, Plattner G-K, Rodgers KB, Sabine CL, Sarmiento JL, Schlitzer R, Slater RD, Totterdell IJ, Weirig M-F, Yamanaka Y, Yool A (2005) Anthropogenic ocean acidification over the twenty-first century and its impact on calcifying organisms. Nature 437: 681–686
Palmqvist K, Yu J-W, Badger MR (1994) Carbonic anhydrase activity and inorganic carbon fluxes in low- and high-C_i cells of *Chlamydomonas reinhardtii* and *Scenedesmus obliquus*. Physiol Plant 90: 537–547
Price GD, Badger MR (1989) Expression of human carbonic anhydrase in the cyanobacterium Synechococcus PCC7942 creates a high CO_2-requiring phenotype. Evidence for a central role for carboxysomes in the CO_2 concentrating mechanism. Plant Physiol 91: 505–513
Raven JA (1997) CO_2 concentrating mechanisms: a direct role for thylakoid lumen acidification? Plant Cell Environ 20: 147–154
Raven JA, Lucas WJ (1985) Energy costs of carbon acquisition. In: Lucas WJ, Berry JA (eds) Inorganic carbon uptake by aquatic photosynthetic organisms. American Society of Plant Physiologists, Rockville, MD, pp 305–324
Raven JA, Johnston AM (1991) Mechanisms of inorganic carbon acquisition in marine phytoplankton and their implications for the use of other resources. Limnol Oceanogr 36: 1701–1714
Rost B, Zondervan I, Riebesell U (2002) Light-dependant carbon isotope fractionation in the coccolithophorid *Emiliania huxleyi*. Limnol Oceanogr 47: 120–128
Rost B, Riebesell U, Burkhardt S, Sültemeyer D (2003) Carbon acquisition of bloom-forming marine phytoplankton. Limnol Oceanogr 48: 55–67
Rost B, Riebesell U, Sültemeyer D (2006a) Carbon acquisition of marine phytoplankton. Effect of photoperiod length. Limnol Oceanogr 51: 12–20
Rost B, Richter K-U, Riebesell U, Hansen PJ (2006b) Inorganic carbon acquisition in red tide dinoflagellates. Plant Cell Environ 29: 810–822
Rost B, Kranz S, Richter K-U, Tortell P (2007) Isotope disequilibrium and mass spectrometric studies of inorganic

carbon acquisition by phytoplankton. Limnol Oceanogr Methods 5: 328–337

Rotatore C, Colman B, Kuzma M (1995) The active uptake of carbon dioxide by the marine diatoms *Phaeodactylum tricornutum* and *Cyclotella* sp. Plant Cell Environ 18: 913–918

Schmidt LE, Hansen PJ (2001) Allelopathy in the prymnesiophyte *Chrysochromulina polylepis*: effect of cell concentration, growth phase and pH. Mar Ecol Prog Ser 216: 67–81

Schulz KG, Rost B, Burkhardt S, Riebesell U, Thoms S, Wolf-Gladrow DA (2007) The effect of iron availability on the regulation of inorganic carbon acquisition in the coccolithophore *Emiliania huxleyi* and the significance of cellular compartmentation for stable carbon isotope fractionation. Geochim Cosmochim Acta 71: 5301–5312

Sharkey TD, Berry JA (1985) Carbon isotope fractionation of algae influenced by an inducible CO_2 concentrating mechanism. In: Lucas WJ, Berry JA (eds) Inorganic carbon uptake by aquatic photosynthetic organisms. American Society of Plant Physiologists, Rockville, MD, pp 389–401

Silverman DN (1982) Carbonic anhydrase. Oxygen-18 exchange catalyzed by an enzyme with rate contributing proton-transfer steps. Methods Enzymol 87: 732–752

Sterling D, Reithmeier RAF, Casey JF (2001) A transport metabolon. J Biol Chem 276: 47886–47894

Sültemeyer D (1998) Carbonic anhydrase in eukaryotic algae: characterization, regulation, and possible function during photosynthesis. Can J Bot 76: 962–972

Thoms S, Pahlow M, Wolf-Gladrow DA (2001) Model of the carbon concentrating mechanism in chloroplasts of eukaryotic algae. J Theor Biol 208: 295–313

Tortell PD, Morel FMM (2002) Sources of inorganic carbon for phytoplankton in the eastern Subtropical and Equatorial Pacific Ocean. Limnol Oceanogr 47: 1012–1022

Tortell PD, DiTullio GR, Sigman DM, Morel FMM (2002) CO_2 effects on taxonomic composition and nutrient utilization in an Equatorial Pacific phytoplankton assemblage. Mar Ecol Prog Ser 236: 37–43

Tortell PD, Martin CL, Corkum ME (2006) Inorganic carbon uptake and intracellular assimilation by subarctic Pacific assemblages. Limnol Oceanogr 51: 2102–2110

Wilbur KM, Anderson NG (1948) Electrometric and colometric determination of carbonic anhydrase. J Biol Chem 176: 147–154

Wolf-Gladrow DA, Riebesell U (1997) Diffusion and reaction in the vicinity of plankton: a refined model for inorganic carbon transport. Mar Chem 59: 17–34

Wolf-Gladrow DA, Riebesell U, Burkhardt S, Bijma J (1999) Direct effects of CO_2 concentration on growth and isotopic composition of marine phytoplankton. Tellus 51: 461–476

Zeebe RE, Wolf-Gladrow DA (2001) CO_2 in Seawater: Equilibrium, Kinetics, Isotopes. Elsevier Science, Amsterdam

Zhang J, Quay PD, Wilbur DO (1995) Carbon isotope fractionation during gas-water exchange and dissolution of CO_2. Geochim Cosmochim Acta 59: 107–114

Edited by V. Hurry